NASA MEMO 10-4-58L

NASA

MEMORANDUM

AN INVESTIGATION OF POSSIBLE DECOY CONFIGURATIONS

FOR INTERCONTINENTAL BALLISTIC MISSILES

By James W. Youngblood and Eugene D. Schult

Langley Research Center
Langley Field, Va.

FACILITY FORM 602

(ACCESSION NUMBER)

31
(PAGES)

(THRU)

(CODE)

(NASA CR OR TMX OR AD NUMBER)

(CATEGORY)

NATIONAL AERONAUTICS AND SPACE ADMINISTRATION

WASHINGTON

October 1958

NATIONAL AERONAUTICS AND SPACE ADMINISTRATION

NASA MEMO 10-4-58L

AN INVESTIGATION OF POSSIBLE DECOY CONFIGURATIONS

FOR INTERCONTINENTAL BALLISTIC MISSILES*

By James W. Youngblood and Eugene D. Schult

SUMMARY

An exploratory investigation has been made of simple configurations suggested as possible decoys for use with ballistic missiles. The study was initiated on the premise that detection of differences in the ballistic trajectory parameter W/C_DA could provide post-reentry discrimination between the warhead, decoys, and scattered components of the parent missile. The decoy geometry necessary to achieve the level of W/C_DA required to elude aerodynamic discrimination was obtained after tunnel and free-flight drag measurements at Mach numbers up to 2 indicated the approximate drag level to be expected at higher speeds. One promising decoy was a 6-leg "jack" consisting of three mutually perpendicular bars. Measurements of the relative radar signal return from a variety of shapes carried aloft by free balloons were obtained with S-band radar at ranges up to approximately 15,000 yards and were used to determine roughly the span and weight requirements.

The limited results indicated that the radar echo area was largely a function of jack span, while W/C_DA was a function only of leg diameter and material density, the higher densities being more efficient for a given weight. The decoy weight penalty for matching present day warheads at S-band frequencies was estimated to be about 300 pounds. For shapes and speeds of operational interest, the drag coefficient of jacks appears to be between the theoretical drag coefficients of a sphere and an infinite transverse circular cylinder and is not greatly affected by the number of legs, leg fineness ratio, or orientation to the free stream.

INTRODUCTION

Inasmuch as the defense of a target complex is critically dependent upon an early identification of the warhead, considerable attention has been focused in recent months on the problem of discriminating between the warhead and the "cloud" of expended fuel tanks, rocket motors, and such items, which may be intentionally scattered early in the trajectory. While reentry aerodynamic heating effects or dispersion of components due to differences in the ballistic trajectory parameter $W/C_D A$ would tend to simplify the problem (fig. 1), the prospect of contending with decoys identical to the warhead in both the radar and trajectory senses could be an overwhelming problem from the standpoint of defense capability.

The purpose of the present investigation is to examine the feasibility of these so-called post-reentry type decoys, as opposed to pre-reentry types, which supposedly could be relatively light and efficient corner reflectors. A decoy with promise for surviving a reentry is a 6-leg decoy (called a jack) consisting of 3 mutually perpendicular bars. At the speeds of interest the drag coefficient of this shape might be expected to correspond to that for a circular cylinder in transverse flow. If so, available high-speed data on cylinders could be used to estimate drag. It can be speculated, however, that some drag alleviation will result from the forward legs, especially at lower Mach numbers and with legs of lower fineness ratio. In order to investigate these premises, free-flight and tunnel measurements were made of the drag of several jack shapes at Mach numbers up to approximately 2. Leg fineness ratio was varied between 4 and 8, and one jack was tested at different orientations to the free stream. The effect of increasing the number of legs to 18 was also explored in the hope of improving both the level of $W/C_D A$ and the radar echo area without adding weight, and also to obtain some indication of the drag characteristics of a severed missile rocket motor which this shape might resemble.

Since the decoy must match the warhead in both the trajectory and radar senses, and since very little data exist on this latter aspect of the detection problem, the present investigation included radar studies of a variety of decoy shapes including jacks, spheres, corner reflectors, and orthogonal rings. These models were carried aloft by free balloons to a maximum slant range of approximately 15,000 yards and viewed with an S-band radar to obtain values of their relative signal returns.

SYMBOLS

A   projected model frontal area, sq ft

b   maximum model span, or twice leg length to center line, in., unless otherwise noted

C_D drag coefficient, $\dfrac{\text{Drag}}{qA}$

d   leg or rod diameter, in.

n   fineness ratio, b/d

g   acceleration due to gravity, ft/sec^2

M   Mach number

q   stream dynamic pressure, $0.7p_\infty M^2$, lb/sq ft

p_∞ stream static pressure, lb/sq ft

t   time, sec

V   velocity along flight path, ft/sec

W   weight, lb

$W/C_D A$ ballistic trajectory parameter determining the terminal dynamic pressure in zero-lift free fall, lb/sq ft

ρ average density of configuration, lb/cu in.

λ wave length of particular S-band radar signal, 4.22 in.

σ radar cross-section area

DRAG INVESTIGATION

Models and Tests

Details of the 4-inch-span jack models tested in free flight are presented in figure 2 and in the photographs of figure 3. Models 1

to 5 were welded from steel round stock of 1/2-, 3/4-, and 1-inch diameter. The two higher speed models 6 and 7 were fabricated from 1-inch steel tubing and filled with lead to alleviate somewhat the high model decelerations that otherwise might be expected. These large decelerations resulted in relatively short test times (by previous standards), and as a check on the technique, repeat tests were made of duplicates of models 1, 3, and 5. Data were obtained on all except the duplicate of model 5.

In the tests of models 1 to 5, one leg of the jack was inserted into a hole in the side of the nose section of a standard 3.25-inch aircraft rocket. The jack was separated in flight by means of a delay squib which ignited a small quantity of black powder. An alternate method was necessary for separating models 6 and 7 from their boosters because of the increased drag at higher Mach numbers. In this method the model was mounted on a pivoted sting attached to the front of a 5-inch HPAG rocket motor. The sting was released and shunted to the side (fig. 3(b)) by means of a powder charge ignited just prior to rocket motor burnout. Ground tests indicated the models were ejected at velocities of approximately 30 feet per second. Some model spin was anticipated from both methods of launching. Visual tracking of only models 6 and 7 was provided by means of approximately 0.02 pound of a smoke-producing chemical stored in one leg of each jack and released through a small orifice at the tip.

The flight tests were conducted at the Langley Pilotless Aircraft Research Station at Wallops Island, Va. The models were accelerated to the maximum test Mach number and then separated from the booster. All test measurements were made during the following 4 seconds of decelerating flight along the ascending portion of the trajectory. A CW Doppler velocimeter was employed to obtain a velocity-time curve which was then differentiated to obtain model deceleration and drag. These measurements and rawinsonde data permitted an evaluation of the Mach number, Reynolds number, dynamic pressure, and total drag coefficient. An attempt to use SCR-584 tracking radar was unsuccessful because of the short time available for identifying the model after separation. Calculated trajectories were therefore relied upon to furnish the necessary altitude information and Doppler velocity corrections due to small (2°) changes in flight path curvature during the tests.

Wind-tunnel tests of jack model 8 at two orientations to the free stream were conducted in the 8-inch preflight jet, also at the Langley Pilotless Aircraft Research Station, Wallops Island. Total drag at $M = 2.03$ was obtained with a hydraulic sting from time histories of hydraulic fluid pressure. As a check on the technique, tests were also made on a 2.5-inch diameter sphere, and results were compared with existing sphere data.

Accuracy

In general the inaccuracies in flight test results are believed to be of the order of ±5 percent in C_D and ±0.02 in Mach number. The estimated inaccuracy of the preflight-jet data for model 8 is ±3 percent in C_D and approximately ±0.02 in Mach number.

Results and Discussion of Drag Investigation

The aerodynamic results of the present investigation are presented in figures 4 to 6. The variation of test Reynolds number per foot with Mach number is shown in figure 4 for both free flight and tunnel tests, and drag results from the flight tests are shown in figure 5. The scatter between supposedly identical configurations is believed to be largely a result of uncertainties in fairing the velocity-time histories. It is possible however that some drag variation in the transonic range may arise as a result of differences between models in the streamwise orientation of the jacks.

Effect of leg fineness ratio.- It might be expected, intuitively, that increased fineness ratio or Mach number would reduce the drag allev- iation produced by the foremost legs and would result in drag coeffi- cients which approach those for a long circular cylinder in transverse flow ($n = \infty$). In figure 5 test results up to $M = 1.2$ for 6-leg jacks of equal spans show some drag alleviation at lower speeds but no con- sistent variation due to fineness ratio in the range between 4 and 8. At $M = 2$ a tendency for the drag coefficient to increase is evident for increases in fineness ratio from 4 to 5.

Effect of jack orientation to stream.- Tests at Mach number 2.03 of a 6-leg jack of fineness ratio 5 in the preflight jet yielded the following drag information:

	A, sq ft	C_D
6-leg jack: 4 legs normal to stream . . . . All legs symmetrically inclined	0.035 0.036	1.17 1.16
$2\frac{1}{2}$ -inch sphere	0.034	0.99

No significant difference in drag is apparent as a result of jack orien- tation to the free stream at this Mach number. In this comparison C_D is based upon the actual projected frontal area and therefore contains

the small area contributions of the angled tips. The sphere test was used primarily to verify the hydraulic sting technique for measuring drag, and is included here only as a matter of casual interest. As is shown subsequently these results agree closely with those of references 1, 2, and 3.

Effect of shape.- Figure 6 compares the drag coefficients of 6- and 18-leg jacks of equal leg diameter and span, together with values for small spheres, a transverse circular cylinder, and a thin flat disk normal to the free stream. The disk calculation comprises the contributions of maximum impact and vacuum base pressure. The difference in jack shape associated with the addition of 12 legs to the original 6 resulted in a considerable increase in drag coefficient at lower test speeds. However, the difference became smaller with increasing speed, and at $M = 2$ amounted to less than 10 percent. On the basis of these results it would appear that the interference effects contribute little to the total drag at high speeds and that at the speeds of interest, the coefficient would probably lie between the theoretical drag coefficient of a sphere and that of a long transverse circular cylinder.

RADAR INVESTIGATION

Due to a general lack of radar information on decoy shapes of current interest, a limited investigation was conducted to determine the radar reflecting properties of these shapes relative to the more conventional spheres and corner reflectors. For this part of the investigation, a total of 22 models were carried aloft on two different days by free balloons and tracked with the S-band radar available at the Pilotless Aircraft Research Station (fig. 7). The models used are shown in figures 8 and 9.

Equipment and Methods for Radar Test

The NACA modified SCR-584, S-band radar was calibrated upon completion of each day's test by inserting a standard signal generator into the receiver circuit at the transformer level and recording AGC (automatic gain control) voltage as a function of the variable output power of the signal generator. Figure 10 shows the resulting calibration curve. Although the noise level of the receiver was seen to vary from day to day, it was still considered justifiable to fair a single curve through the two sets of calibration points, since readings of AGC voltage were only accurate to 1/10th volt over a full-scale range of five volts.

The free-balloon tests were conducted on October 22, 1957 (test 1), and December 16, 1957 (test 2). Each model was suspended at the end of a 20-foot cotton cord attached to a rubber radiosonde balloon and after balloon launch was tracked by radar until the return signal faded out, or until some pre-determined range was attained. Readings of AGC voltage were recorded at 2,000-yard increments in slant range. These readings were taken as basic indications of the absolute values of the signal received from each target. The voltage readings were compared with the receiver noise level by using the calibration curve and are plotted in figure 11 as decibels above receiver noise against range. This method of presentation was preferred since it resulted in less scattering of points, and since a straight line having the 4th power slope of the radar equation (ref. 4, pp. 316 and 473) could be faired through the best-fit region of points.

The observed scatter about the faired lines is believed to result from (1) the interference (or ground clutter) through which the models were tracked, (2) small, cumulative inaccuracies in radar operating variables (antenna gain, power output, or noise level), and (3) the fact that the characteristic dimensions of the targets were small compared with the wave-length of the S-band radar (4.22 in.). It was noted, however, that within the limits of tracking range imposed by the small target dimensions, the relative scattering of points generally decreased with increasing range. This effect can best be seen in the case of the larger, more efficient reflectors.

It was also evident that any attenuation contributed by the balloon-string combination alone had vanished at about 6,000-yards range. For this reason, and because of the apparent range effect just described, the graphs of figure 11 were faired by favoring the higher ranges.

Results and Discussion of Radar Investigation

Effect of shape.- The results are summarized in the bar-graph of figure 12, which is intended to convey relative rather than absolute information. The chart reflects, within the accuracy of these tests, the relative radar cross sections of the target models at a range of 8,000 yards. This range was arbitrarily selected because of the absence of balloon attenuation, and because of the range effect referred to previously. From this figure it is evident that for the groups of targets of equal span, the return signal (and hence the radar area) was a maximum for the corner reflector and decreased in turn for the 3-ring decoy, the sphere, the 18-leg jack, and 6-leg jacks.

The ratio of radar area σ to that of a sphere of equal span σ_{sphere} is also given in figure 12. A consistent variation in $\left(\dfrac{\sigma}{\sigma_{sphere}}\right)$

is noted among the 2-, 4-, and 10-inch-span models. Relative to the radar area of the sphere of equal span, the radar area of the corner reflector was roughly twice as large, whereas that of the jacks was only about one-half as large. Although the 4-leg jack was not investigated, its geometry suggests that as a radar reflector, it would be somewhat inferior to the 6-leg jack.

Effect of span.- Although signal level was affected by both leg fineness ratio and decoy span, the span appeared to exert the predominant influence. The resultant variation of signal level with span is evident from figure 12.

Effect of leg fineness ratio.- A definite increase in signal level was noted with increased leg fineness ratio in the case of the 10-inch jacks of radar test 2 (fig. 11(d)). However, although theory predicts it (ref. 4, pp. 350-352, 471-473), the effect was not noticeable with the small jacks of radar test 1 (fig. 11(c)). Since span appeared to be the most influential dimension, the small dimensions of the jacks in test 1 probably nullified any observable fineness-ratio effects.

Effect of heating.- Reentry environmental conditions can be expected to modify the reflecting characteristics of these configurations. In an effort to determine whether radar reflectivity is affected by a thin, hot ($\approx 3,000^\circ$ F) boundary layer, model 29 (a 10-inch base-diameter 90° cone) was fitted with a T-121 magnesium flare inside the cone, and was elevated to altitude by a balloon. The model is shown in figure 10(b) with the flare removed. The model was tracked to 4,000 yards at which time the flare was ignited automatically with a simple timer device. The hot gases from the flare exhausted downward through the apex into a small deflector cup displaced 1/4 inch from the cone body, and then expanded up around the sides of the cone. No change in radar-signal level was noted during the 15-second burning period of the flare, although a 16-millimeter film record indicated that the extent of the flame area was roughly three times the diameter of the cone. The disappearance of the signal shortly after burnout indicated that the model may have failed under the influence of the extremely hot gases.

DECOY MATCHING STUDIES

Range of $W/C_D A$

On the assumption of a drag coefficient of 1.25 based on frontal area, which corresponds to that for a transverse cylinder at high speeds, estimates were made of the $W/C_D A$ range provided by various shapes and materials. The results, together with the equations for four selected
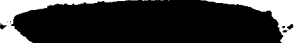
configurations, are summarized in figure 13, where W/C_DA is plotted as a function of leg or rod diameter. The curves of constant weight per unit span involve a slight approximation (usually less than 10 percent for $n \geqq 5$) due to the effect of leg fineness ratio predicted in the weight equation. Since W/C_DA is relatively unaffected by fineness ratio, it is virtually independent of span and is thus a function only of rod diameter and density. In general the weight varies directly as the square of W/C_DA for a given span and density, and inversely with density for a given span and W/C_DA. It also follows that for a given W/C_DA and density, the weight increases directly with span or with radar echo area provided the latter varies proportionally with the span.

In addition to the weight penalties associated with the use of conventional materials, serious space limitations associated with leg diameter may also arise, particularly if W/C_DA levels of the order of 200 are attempted. For the 3-ring decoy (fig. 13(d)) and the 4- and 6-leg jack configurations (figs. 13(a) and (b)), however, some storage space might be saved by resorting to folding techniques. In the interest of weight saving and storage-space economy, the simplest and most efficient shape appears to be the 4-leg jack.

Matching Considerations

It may be expected that the physical properties of the decoy will ultimately depend on the degree of refinement necessary in matching the warhead to assure a reasonable deception and a commitment by the defense to engage all likely targets. The minimum matching requirements are therefore related to the traffic level and to the discriminatory capability of the defense radar both before and during missile reentry. Presumably an ideal match could be obtained by varying the decoy span, once the level of W/C_DA is established by leg diameter and density.

The present tests indicated that the signal return from the post-reentry shapes of interest was usually less than but of the same order of magnitude as that from spheres of equal span. Only the corner reflectors and the 3-ring decoy exhibited stronger signals. On the strength of these results the following table was prepared:

Configuration	Dimensional scale factor relative to sphere
Sphere	1.0
Corner reflector	.4
3-ring decoy	.8
18-leg jack	1.5
6-leg jack	2.0

The scale factor has been assumed to vary inversely as the ratio $\dfrac{\sigma}{\sigma_{sphere}}$ obtained from figure 12, although it is recognized that the variation is not necessarily linear with either changes in dimensions or radar frequency. Thus, the scale factor determines the necessary characteristic dimension for a particular configuration in order that its radar area equal that of a reference sphere.

On the assumption that spheres present roughly the same radar area as oncoming blunt warheads, it might be inferred that decoy and warhead spans should be related according to the foregoing scale factor. In this case the scale factor could be applied to determine the optimum decoy configuration necessary to obtain radar simulation upon reentry. Accordingly, a 6-leg jack, which for the same radar area as the warhead would be larger in span by a factor of 2, was matched to several hypothetical warhead designs to obtain a final weight penalty (fig. 14). It can be seen that decoy weights of the order of 300 pounds could easily result from an ideal match in radar area and $W/C_D A$.

The 6-leg jack as shown here does not necessarily represent the minimum weight configuration for a particular simulation. Brief calculations indicate that the other decoys would also require weights of the order of 300 pounds for a similar case.

CONCLUSIONS

An investigation was made of several post-reentry types of ballistic missile decoy configurations. Drag measurements were obtained from a number of jacks at Mach numbers between approximately 0.6 to 2.0 in order to provide qualitative indications of the differences in drag which might be expected from simple variations in geometry and Mach number. Limited information on the radar reflectivity of jacks, corner reflectors, and spheres was obtained with available S-band radar. Conclusions indicated are:

1. The drag coefficients of the jacks are between the theoretical drag coefficients of spheres and transverse circular cylinders at high speeds.

2. The number of legs, the leg fineness ratio, and the streamwise orientation of the jacks have less influence on the total drag at high speeds than at low transonic speeds. Near Mach number 2, the variation is less than 10 percent, and at still higher speeds would be expected to be even less.

3. For the targets tested with S-band radar, the return signal, and hence the radar echo area, decreased in turn with the 3-ring decoy, the sphere, the 18-leg jack, and the 6-leg jack. For the jacks the return signal varied predominantly with span.

4. For fineness ratios greater than 5, the ballistic trajectory parameter W/C_DA of a jack was independent of span, but increased with increases in material density and leg diameter.

5. Once the level of W/C_DA has been established by the leg diameter and material density, the jack return signal can be matched with the warhead signal merely by varying the span.

6. For W/C_DA approaching 200 the weight of a 6-leg jack decoy could be about 300 pounds.

For specific application, further tests are needed to determine the effects of actual environmental conditions on the radar characteristics of these configurations.

Langley Research Center,
    National Aeronautics and Space Administration,
        Langley Field, Va., July 24, 1958.

12

REFERENCES

1. Hoerner, Sighard F.: Aerodynamic Drag. Published by the Author. (148 Busteed, Midland Park, N. J.), 1951.

2. Hodges, A. J.: The Drag Coefficients of Very High Velocity Spheres. Jour. Aero. Sci., vol. 24, no. 10, Oct. 1957, pp. 755-758.

3. Penland, Jim A.: Aerodynamic Characteristics of a Circular Cylinder at Mach Number 6.86 and Angles of Attack up to 90°. NACA TN 3861, 1957.

4. Burrows, Chas. R., chm., and Attwood, Stephen S., ed.: Radio Wave Propagation. Consolidated Summary Technical Report of the Committee on Propagation of the National Defense Research Committee. Academic Press, Inc. (New York), 1949.
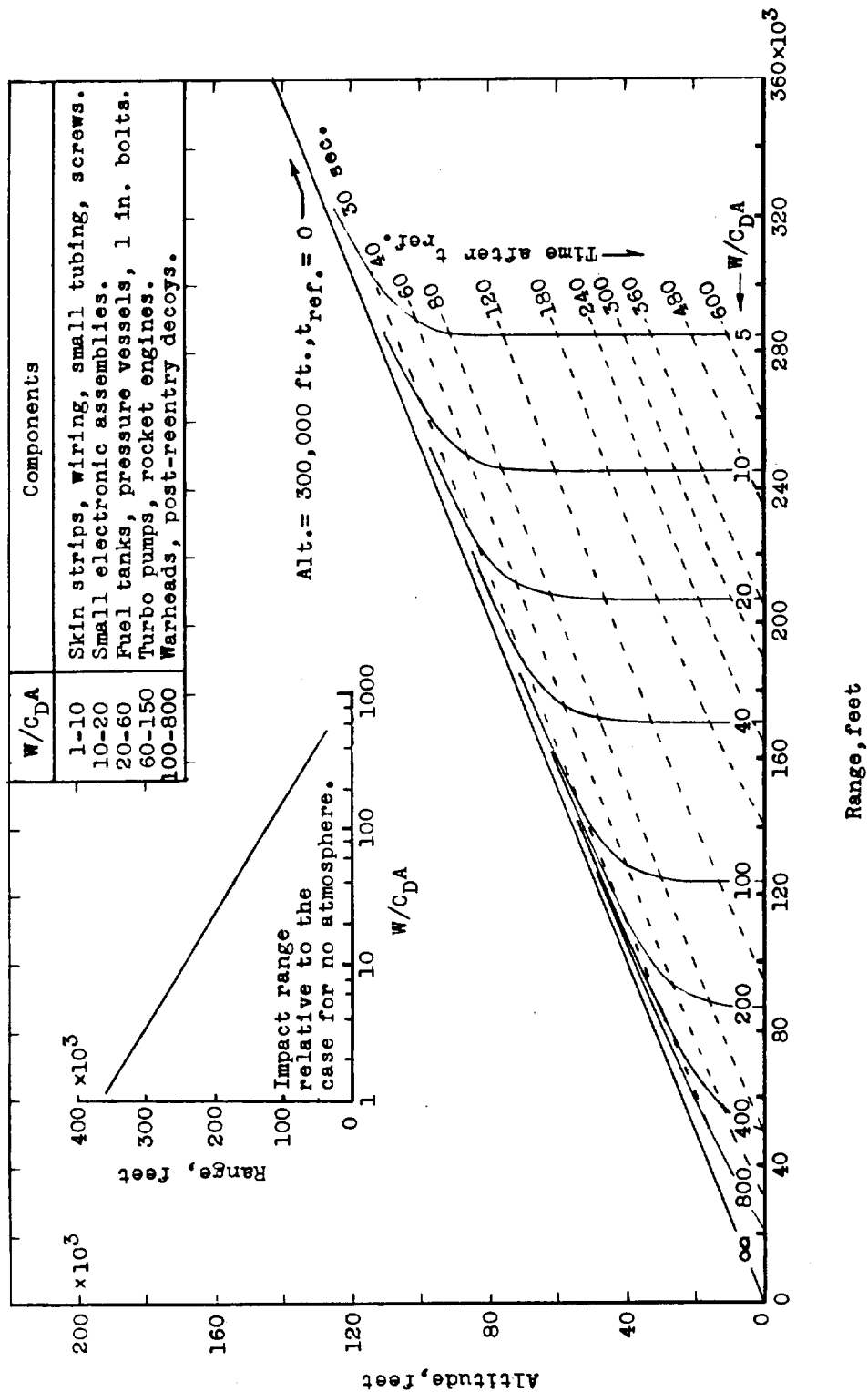
W/C_DA	Components
1-10	Skin strips, wiring, small tubing, screws.
10-20	Small electronic assemblies.
20-60	Fuel tanks, pressure vessels, 1 in. bolts.
60-150	Turbo pumps, rocket engines.
100-800	Warheads, post-reentry decoys.

Alt.= 300,000 ft., $t_{ref.}$ = 0

Time after $t_{ref.}$

30 sec.
40
60
80
120
180
240
300
360
480
600

W/C_DA

5
10
20
40
100
200
400
800
∞

Range, feet

Altitude, feet

200 ×10³
160
120
80
40
0

0   40   80   120   160   200   240   280   320   360×10³

Impact range relative to the case for no atmosphere.

Range, feet

400 ×10³
300
200
100
0

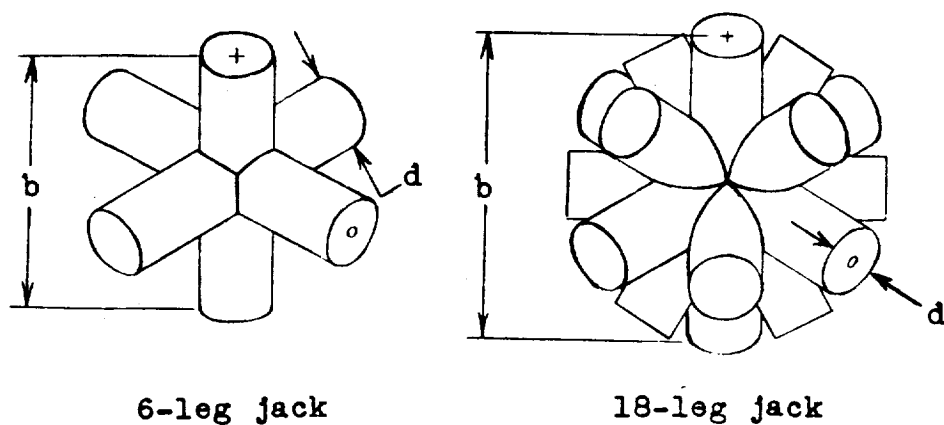W/C_DA

1   10   100   1000

Figure 1.- Estimated fallout time and trajectories of ballistic missile components. Missile range of 5,500 nautical miles; V_{entry} = 23,285 fps at 300,000 feet; entry angle = 21.64°.

6-leg jack   18-leg jack

Model	No. of legs	b, in.	d, in.	n	W, lb
1	6	4	1	4.0	2.392
2	6	4	1	4.0	2.370
3	6	4	3/4	5.33	1.408
4	6	4	3/4	5.33	1.388
5	6	4	1/2	8.0	.659
6	6	4	1	4.0	2.900
7	18	4	1	4.0	7.190
8	6	3.75	3/4	5.0	-----

Figure 2.- Details of jacks used in aerodynamic drag investigations.
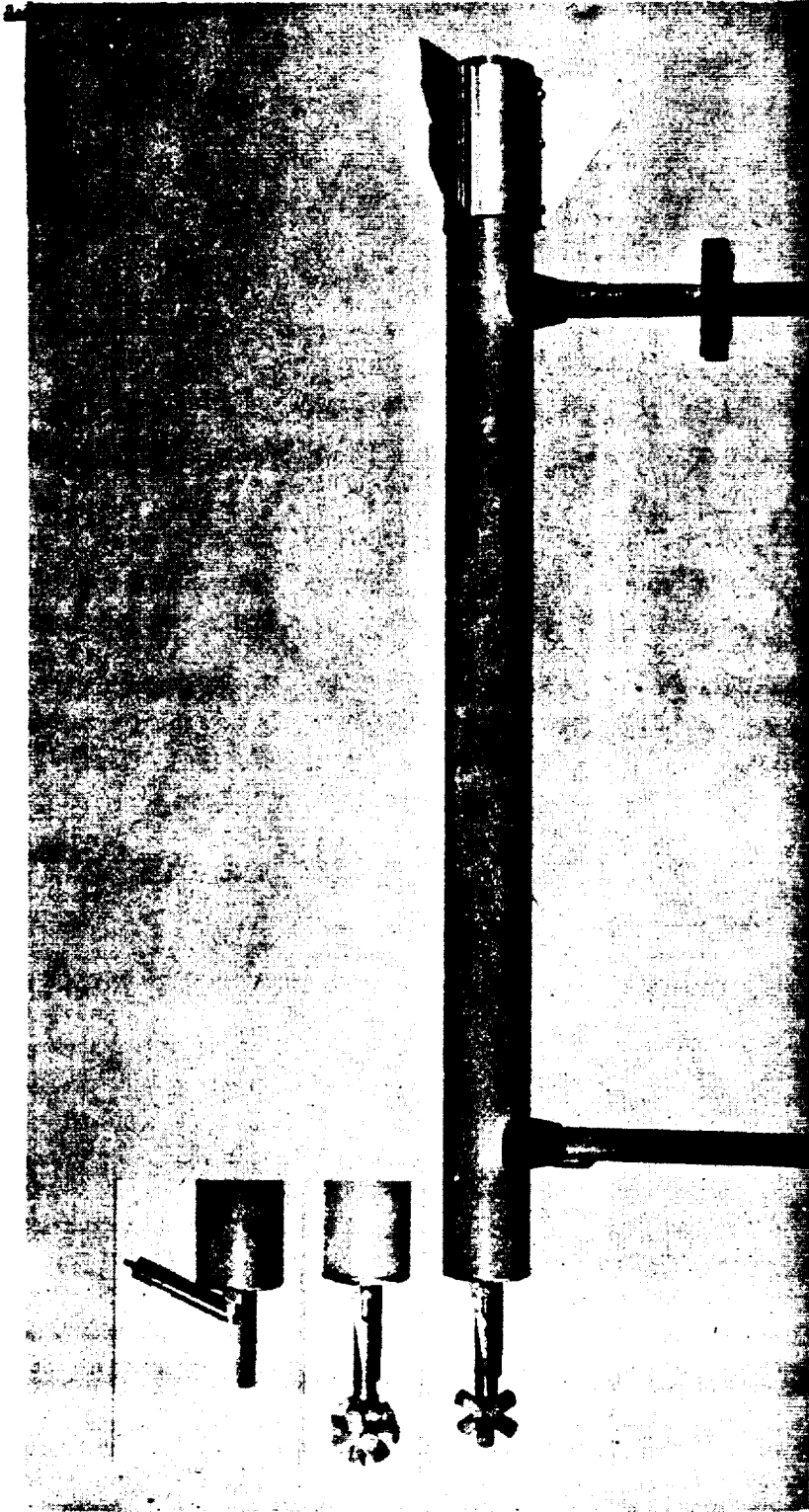
NOT REPRODUCIBLE
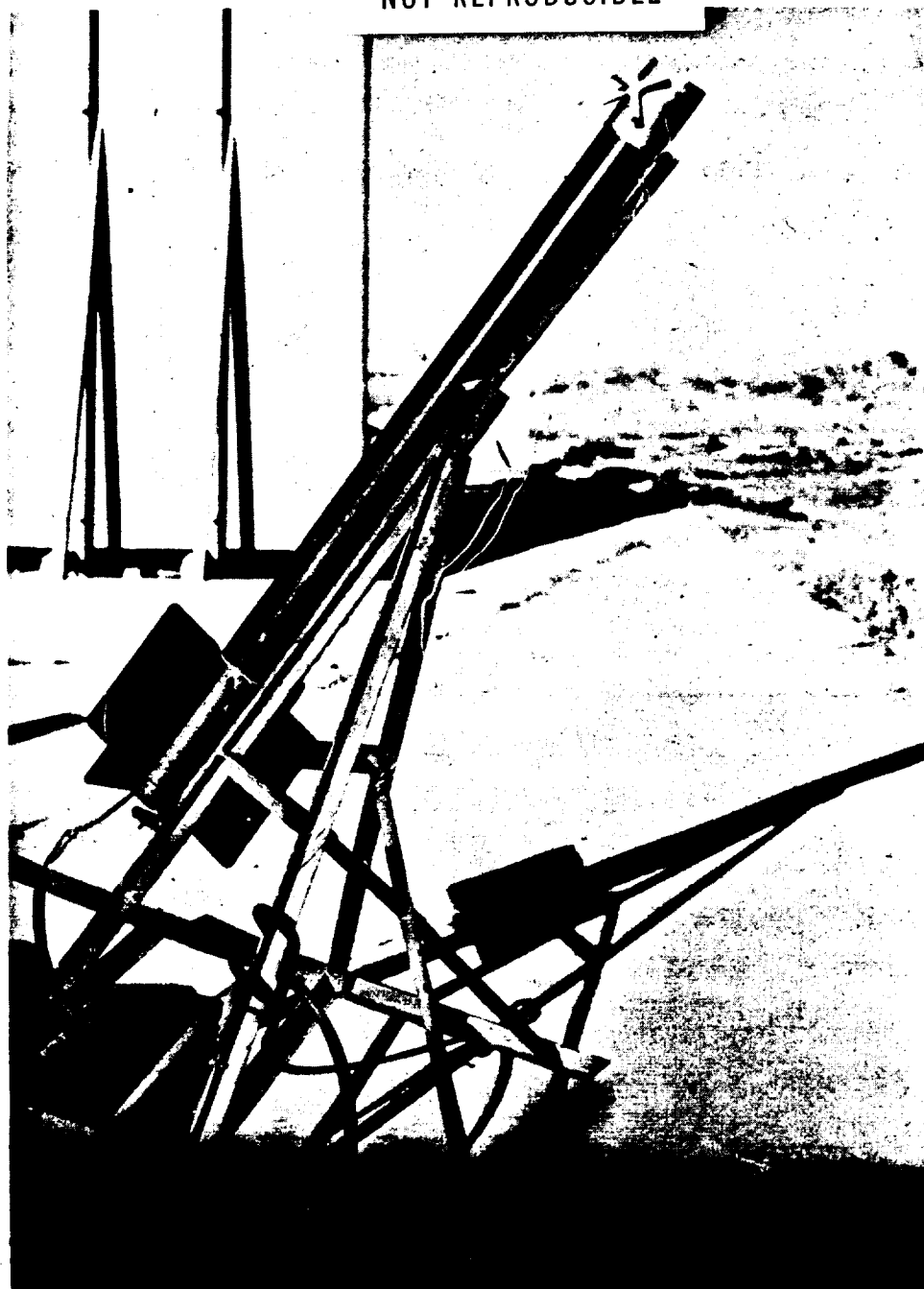
L-57-4633

(a) Model 5 shown on 3.25-inch aircraft rocket prior to flight test.

Figure 3.- Photographs of test vehicles employed for drag determination.

L-58-2522

(b) Model 6 on the HPAG rocket motor. Insets show model 7 and position of launching sting after separation.

Figure 3.- Concluded.
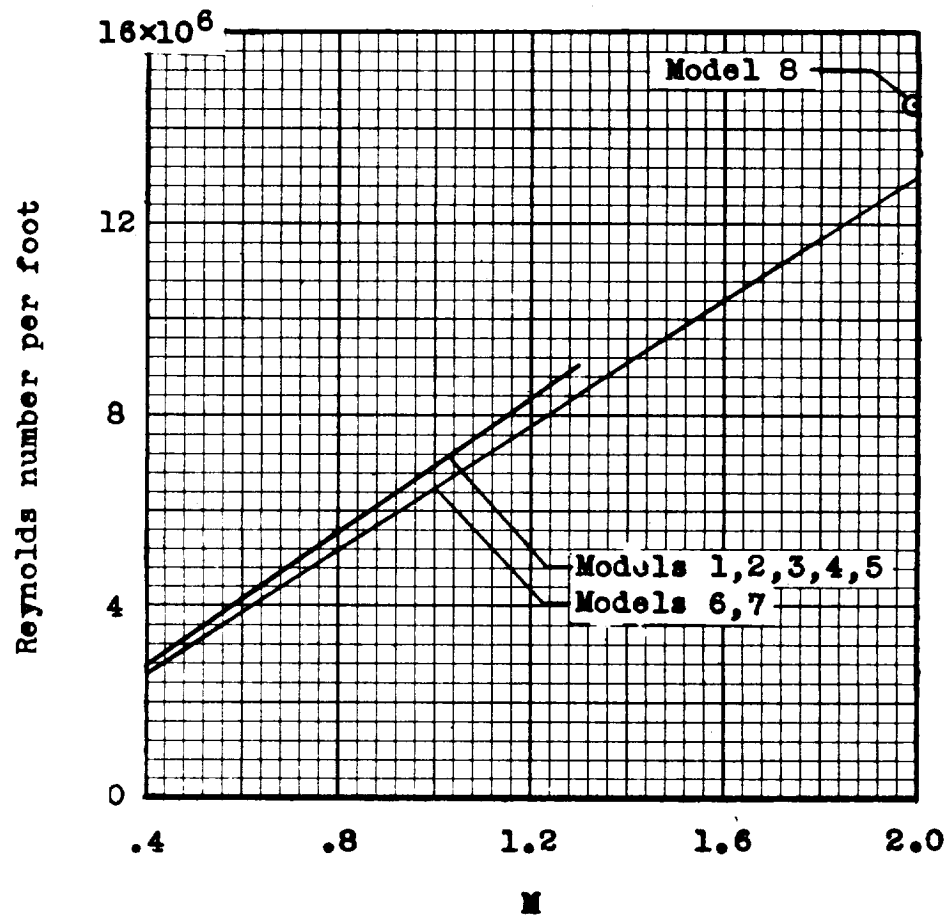
Figure 4.- Variation of Reynolds number with Mach number.
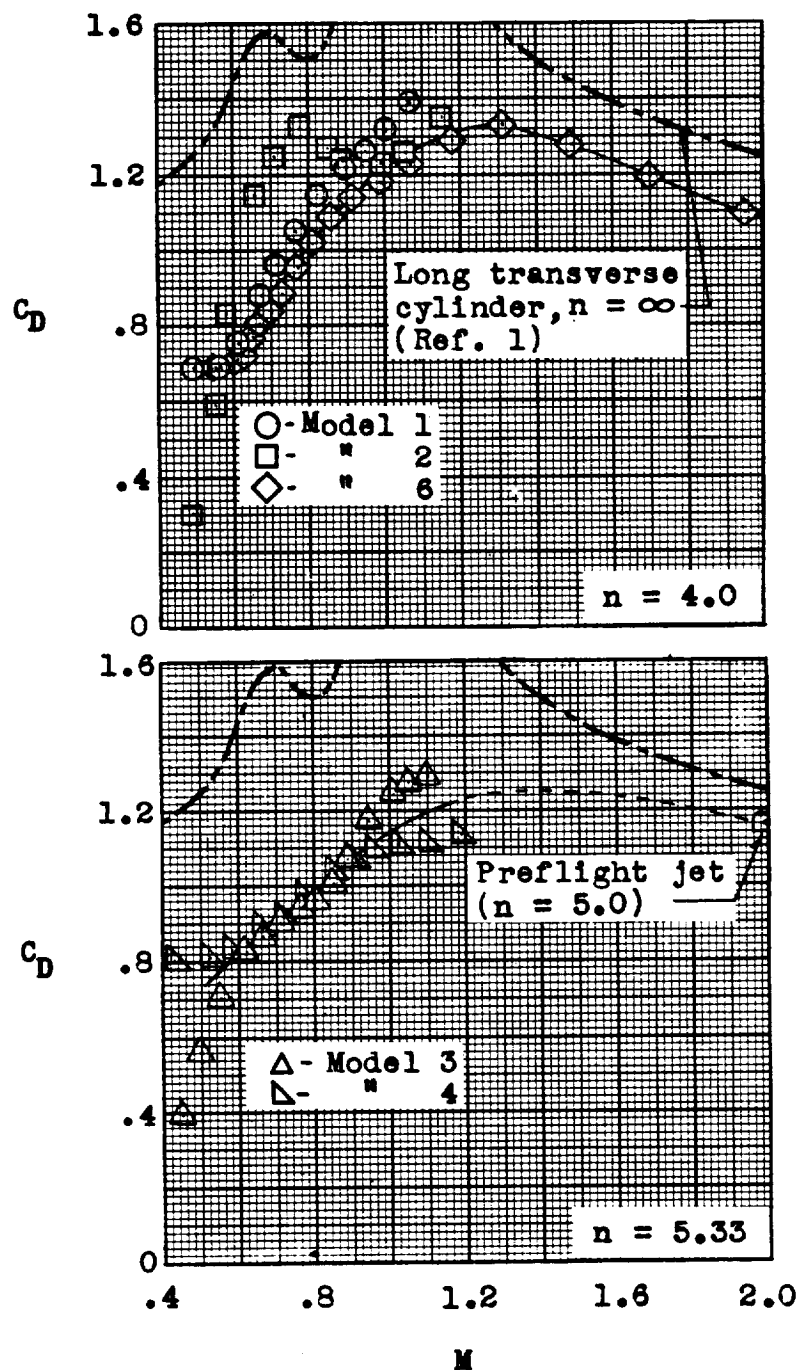
Figure 5.- Variation of drag coefficient with Mach number for long
transverse cylinder (ref. 1) and for 6-leg jacks having different
leg fineness ratios (present test).

Figure 5.- Concluded.
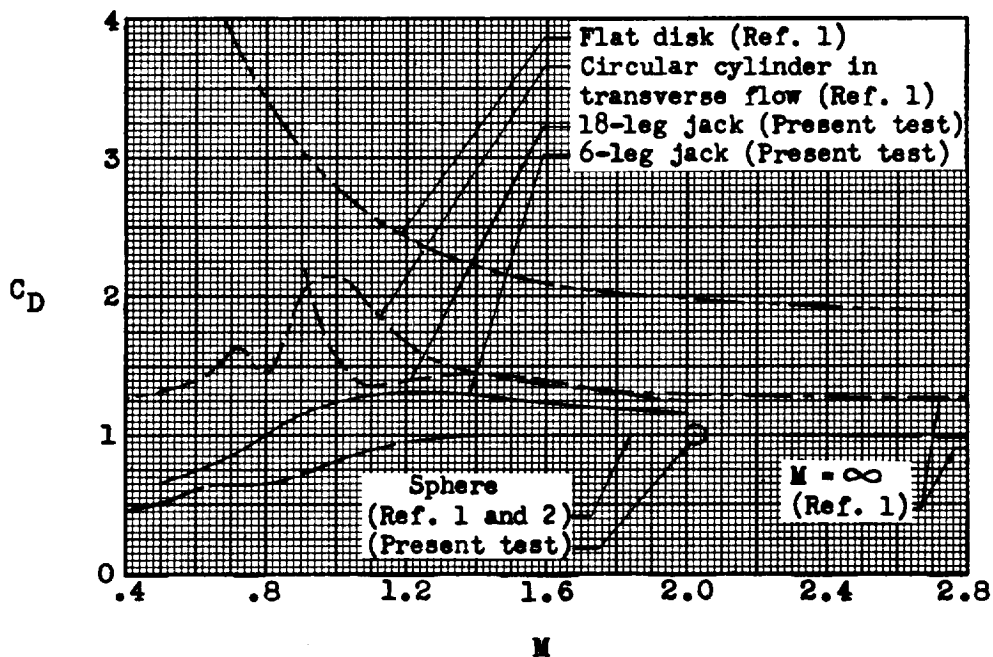
Figure 6.- Variation of drag coefficient with Mach number; comparison
of present test data with reference data.
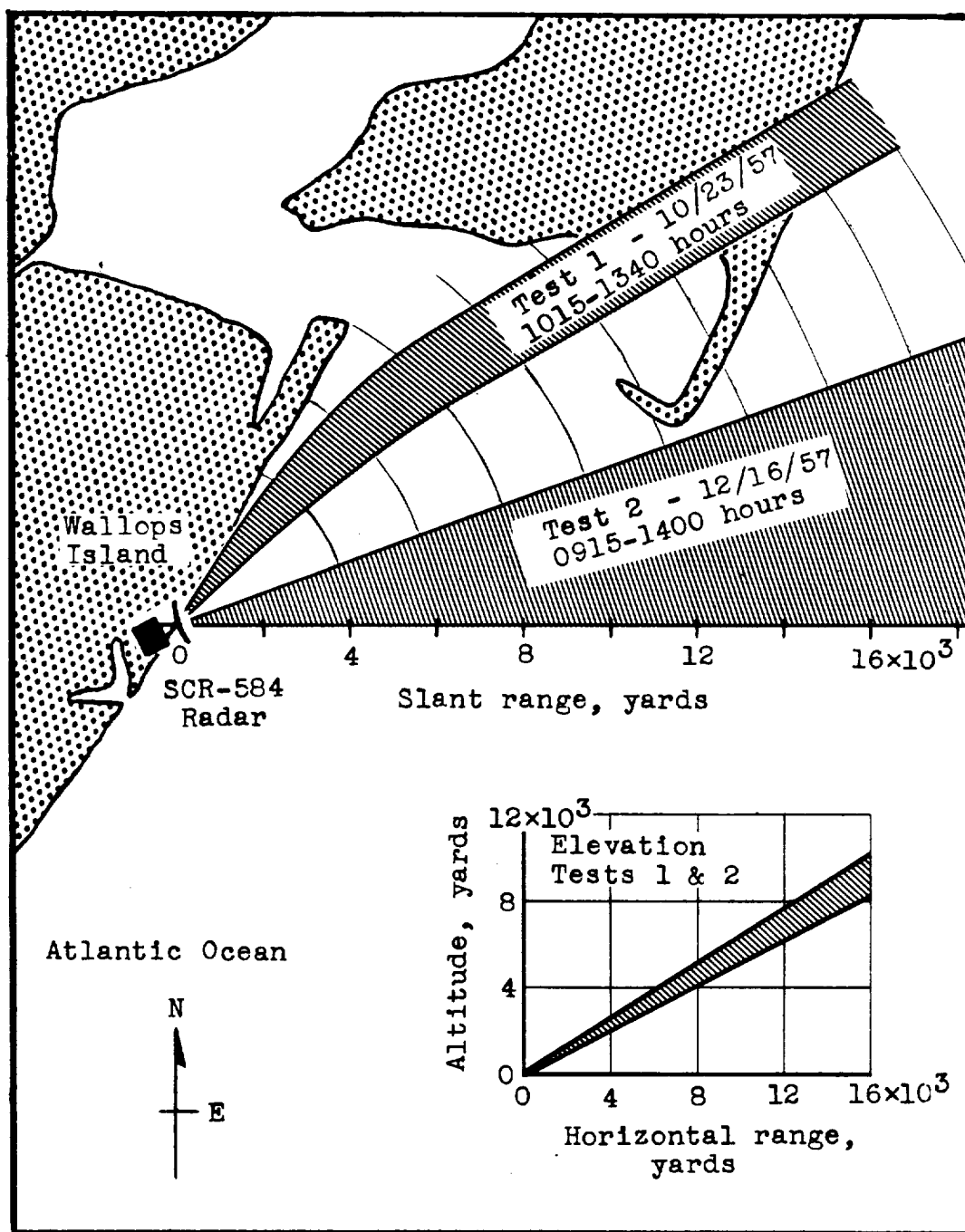
Figure 7.- Range of azimuth and elevation trajectories for the balloon-decoy target combinations launched from the Wallops Island test facility.

Test 1 models

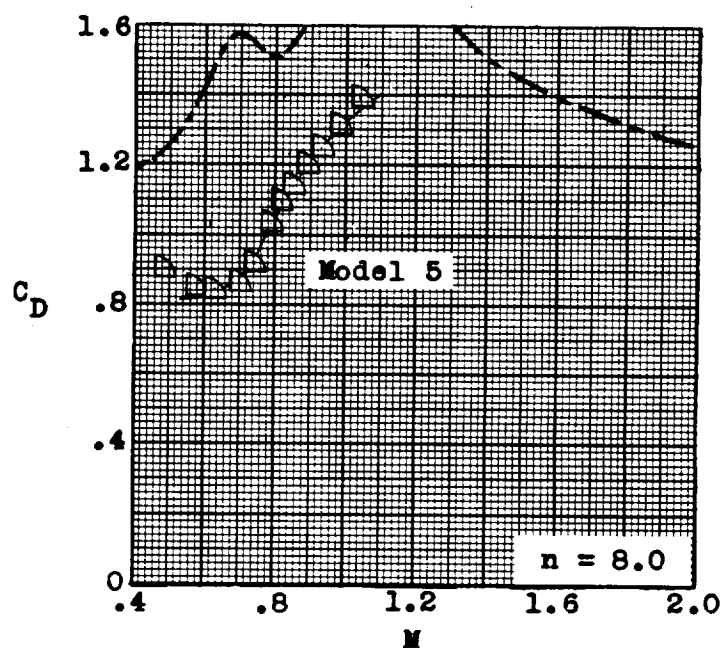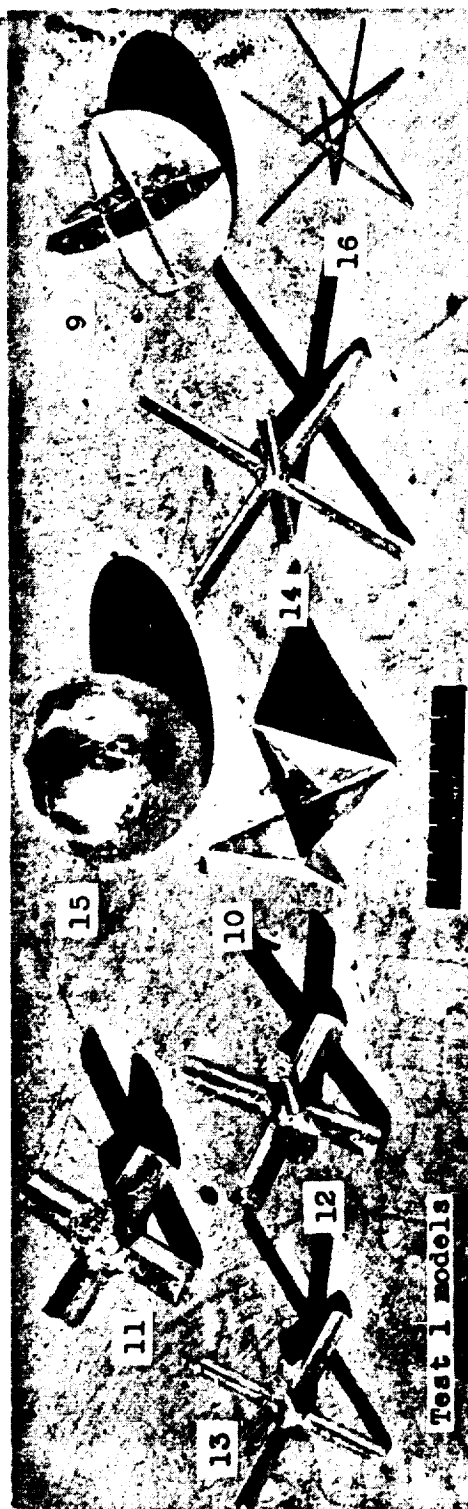| Model (a)	Configuration	b, in.	d, in.	n	b/λ	b/2λ
9	Round corner reflector	4.0	---	---	0.95	0.47
10	Square corner reflector	4.0	---	---	.95	.47
11	6-leg jack	4.0	0.9	4.4	.95	---
12	6-leg jack	4.0	.6	6.7	.95	---
13	6-leg jack	4.0	.36	11.1	.95	---
14	6-leg jack	6.0	.36	16.7	1.42	---
15	Sphere	4.0	---	---	---	.47
16	6-leg jack	4.0	.10	40.0	.95	---

[a]Models 9 to 15 were of aluminum-foil-covered wood or cardboard construction. Model 16 was made of steel rod.

Figure 8.- Radar targets investigated in first free-balloon tests. L-58-2523

Test 2 models
29 & 30 not shown
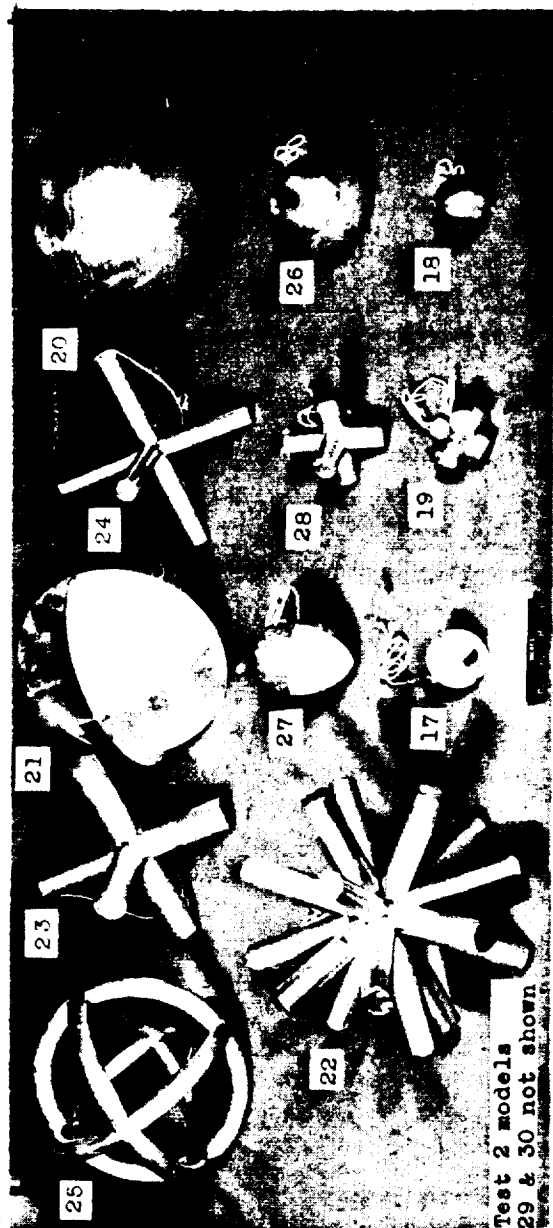
Model (a)	Configuration	b, in.	d, in.	n	b/λ	$b/2\lambda$
17	Round corner reflector	2.0	---	---	0.47	0.24
18	Sphere	2.0	---	---	---	.24
19	6-leg jack	2.0	1.0	2.0	.47	---
20	Sphere	10.0	---	---	---	1.19
21	Round corner reflector	10.0	---	---	2.38	1.19
22	18-leg jack	10.0	1.0	10.0	2.38	---
23	6-leg jack	10.0	1.5	6.7	2.38	---
24	6-leg jack	10.0	1.0	10.0	2.38	---
25	3-ring decoy reflector	10.0	1.0	10.0	2.38	1.19
26	Sphere	4.0	---	---	---	.47
27	Round corner reflector	4.0	---	---	.95	.47
28	6-leg jack	4.0	1.0	4.0	.95	---
29	10-inch, 90° cone with flare	10.0	---	---	2.38	1.19
30	Square corner reflector	34.0	---	---	8.06	4.03

aModels 17 to 30 were of aluminum tubing or sheet construction.

(a) Models 17 to 28.

L-58-2524

Figure 9.- Radar targets investigated in second free-balloon tests.

Top view
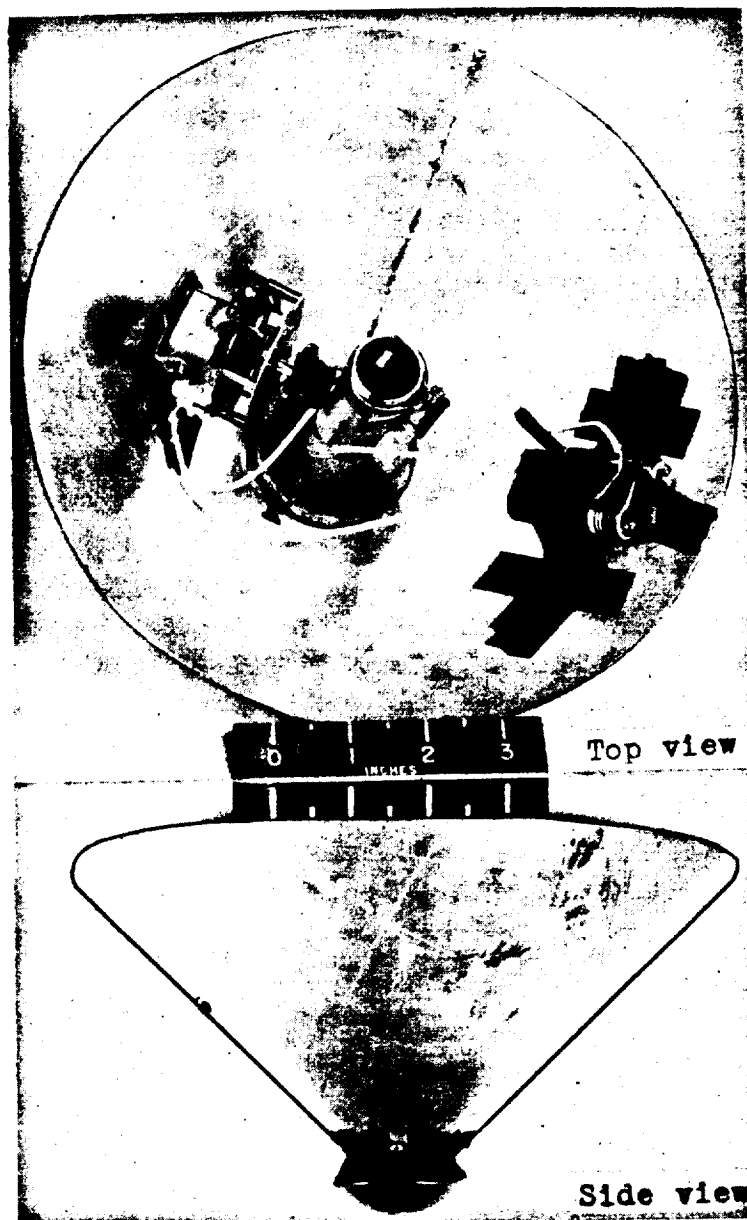
Side view

L-58-2525

(b) Details of model 29; T-121 magnesium flare removed; side view shows
model attitude during test.

Figure 9.- Concluded.
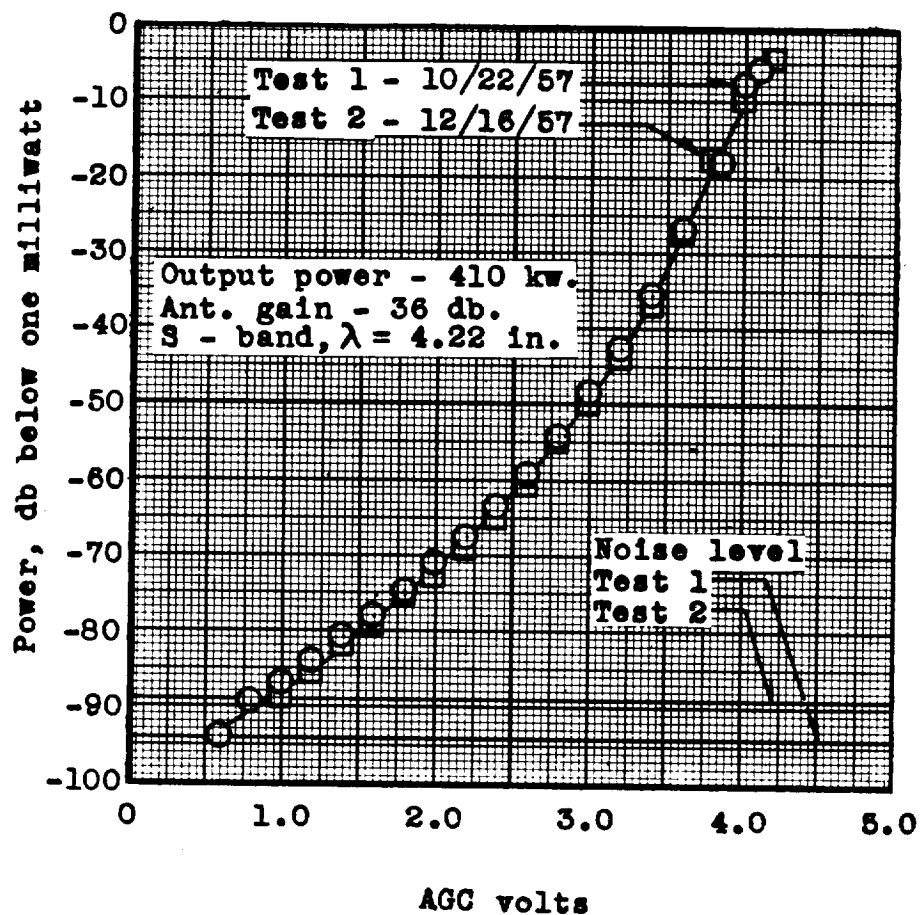
Figure 10.- Calibration curve of NACA modified SCR-584 radar for two different test days.

(b) Corner reflectors.

Model	Shape	b	b/2λ
30	Square	34	4.03
21	Round	10	1.19
9,27	Round	4	.47
10	Square	4	.47
17	Round	2	.24
Balloon & string only			

Range, yards

(a) Spheres.

Model	b	b/2λ
20	10	1.19
15,26	4	.47
18	2	.24
Balloon & string only		

Range, yards

Signal strength, db above noise
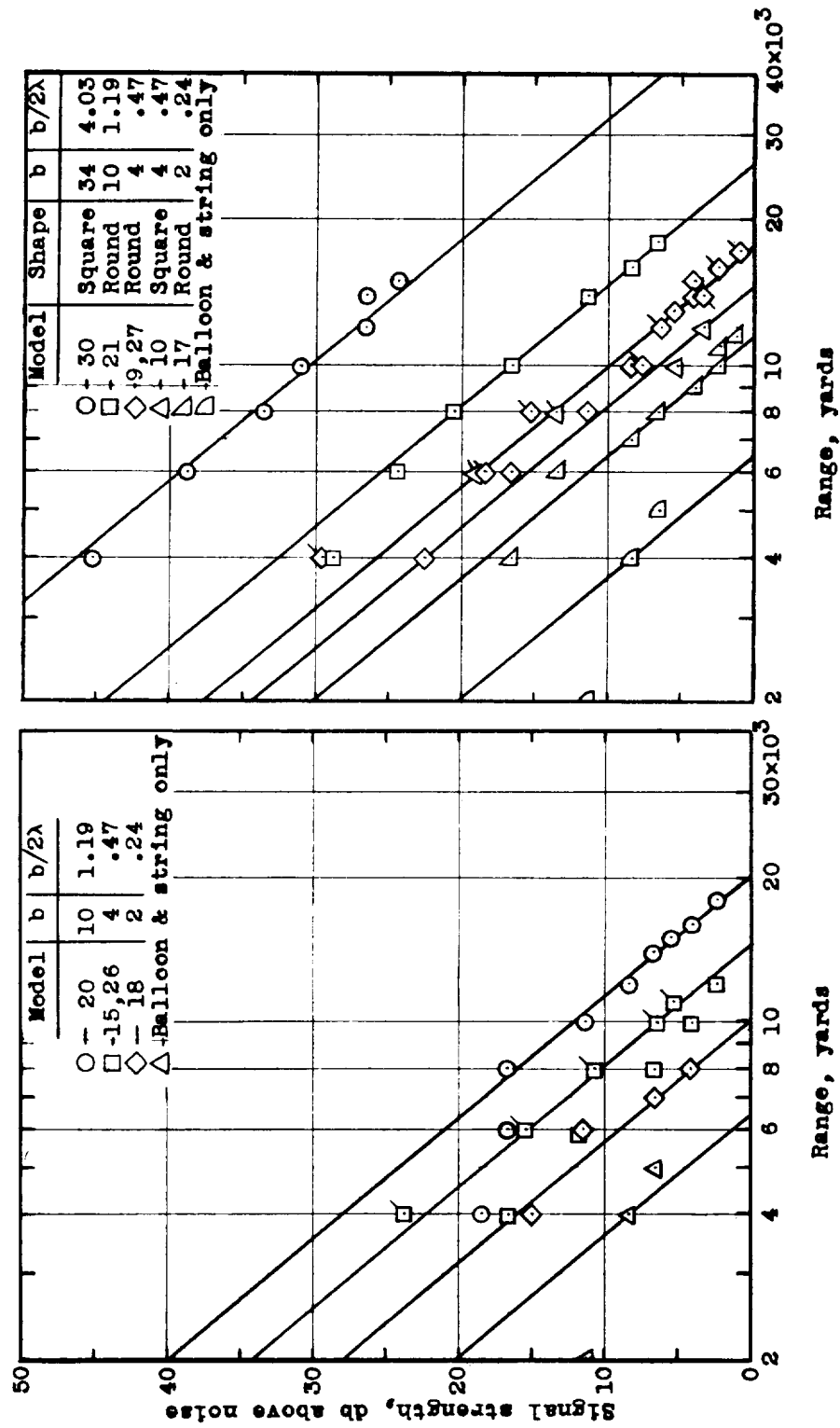
Figure 11.- Variation of received signal strength with range, based on receiver noise level. Flagged symbols indicate data obtained in test 1; λ = 4.22 inches.

Model	b	d	n	b/λ	No. legs
O – 22	10	1.0	10.0	2.38	18
□ – 24	10	1.0	10.0	2.38	6
◇ – 23	10	1.5	6.7	2.38	6
◁ – 28	4	1.0	4.0	.95	6
◁ – 19	2	1.0	2.0	.47	6
⌂ – Balloon & string only					

Range, yards

(d) Jacks, test 2.

Model	b	d	n	b/λ	No. legs
O – 14	6	.36	16.7	1.42	6
□ – 11	4	.90	4.4	.95	6
◇ – 12	4	.60	6.7	.95	6
◁ – 13	4	.36	11.1	.95	6
◁ – 16	4	.10	40.0	.95	6
⌂ – Balloon & string only					

Range, yards

Signal strength, db above noise
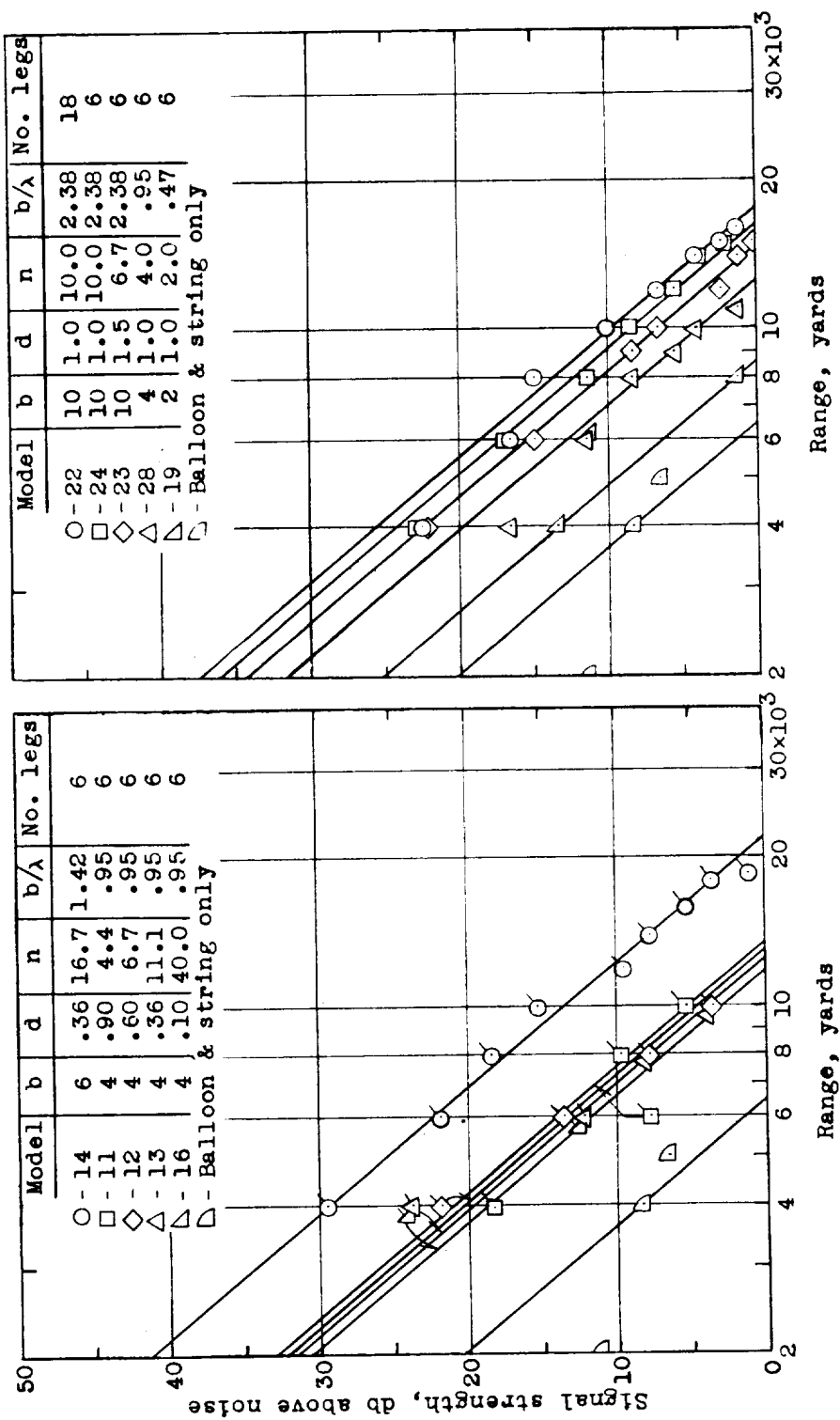
(c) Jacks, test 1.

Figure 11.– Continued.
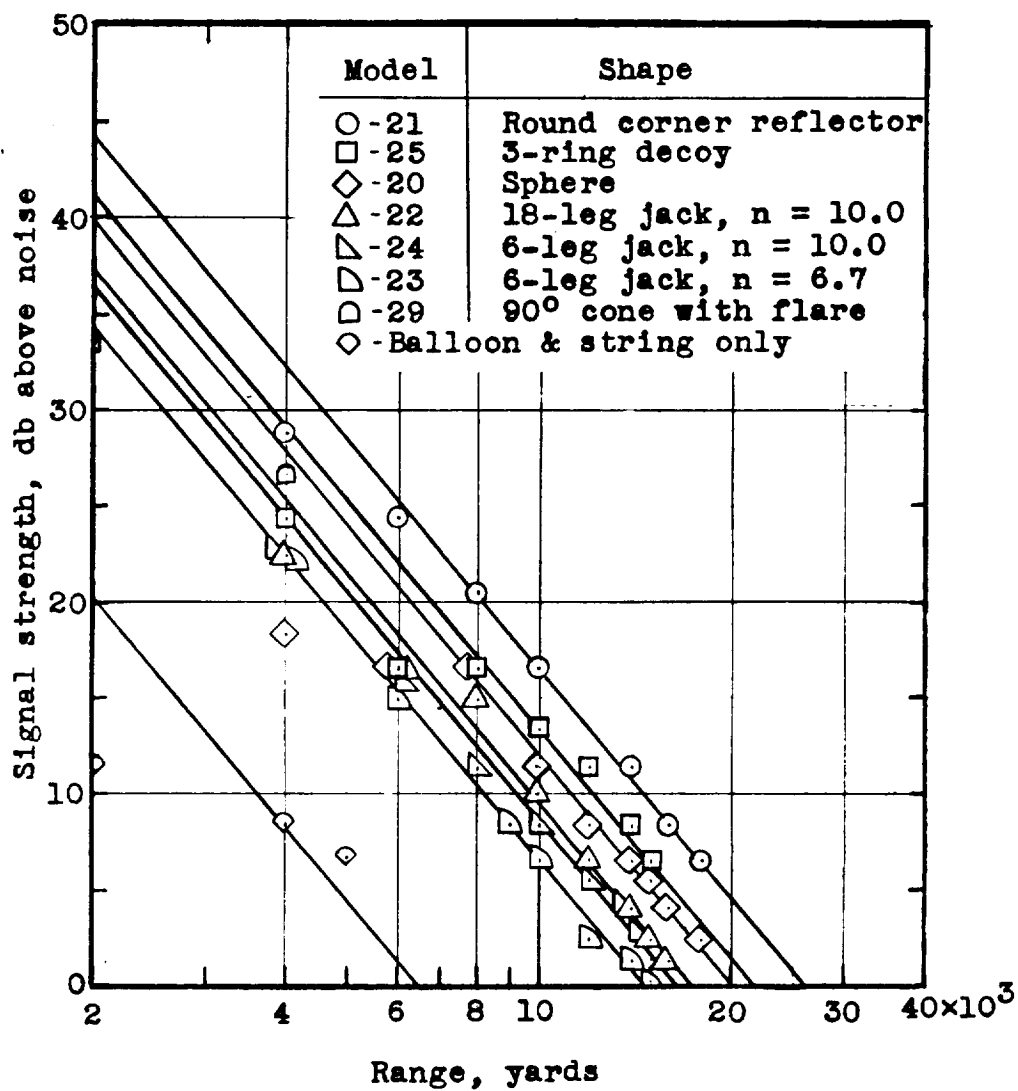
(e) 10-inch models.

Figure 11.- Concluded.

Model	Configuration[1]	b,in.	n		$\dfrac{\sigma}{\sigma_{sphere}}$
30	Square CR	34	—		
21	Round CR	10	—		2.82
25	3-ring "gimbal"		—		1.26
20	Sphere		—		1.00
22	18-leg jack		10.0		.56
24	6-leg jack				.40
23	6-leg jack		6.7		.28
14	6-leg jack	6	16.7		
9,27	Round CR	4	—		2.14
10	Square CR		—		1.08
15,26	Sphere		—		1.00
11	6-leg jack		4.4		.76
12	6-leg jack		6.7		.65
13	6-leg jack		11.1		.56
16	6-leg jack		40.0		.45
17	Round CR	2	—		1.32
18	Sphere		—		1.00
19	6-leg jack		2.0		.53

[1]CR is used for corner reflector.

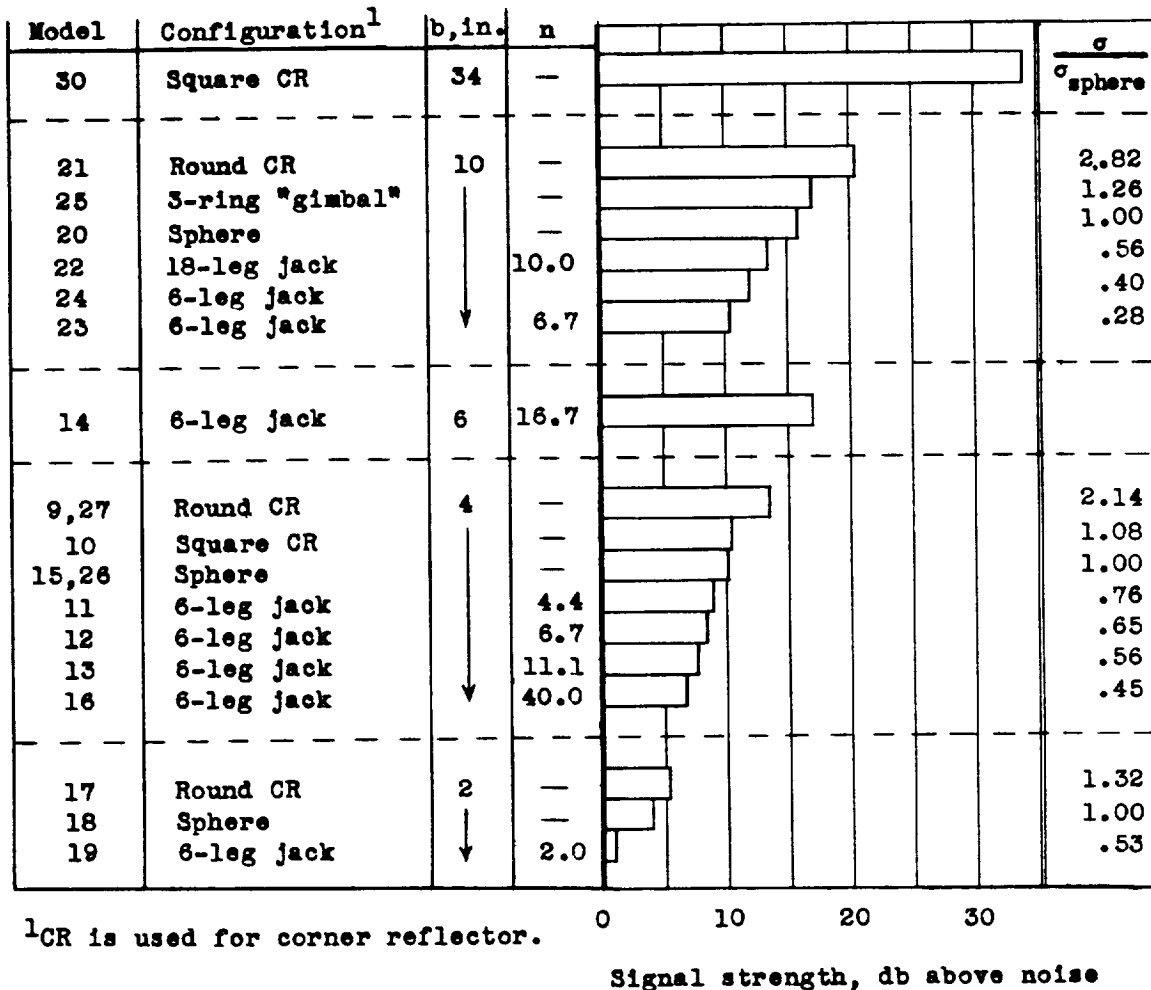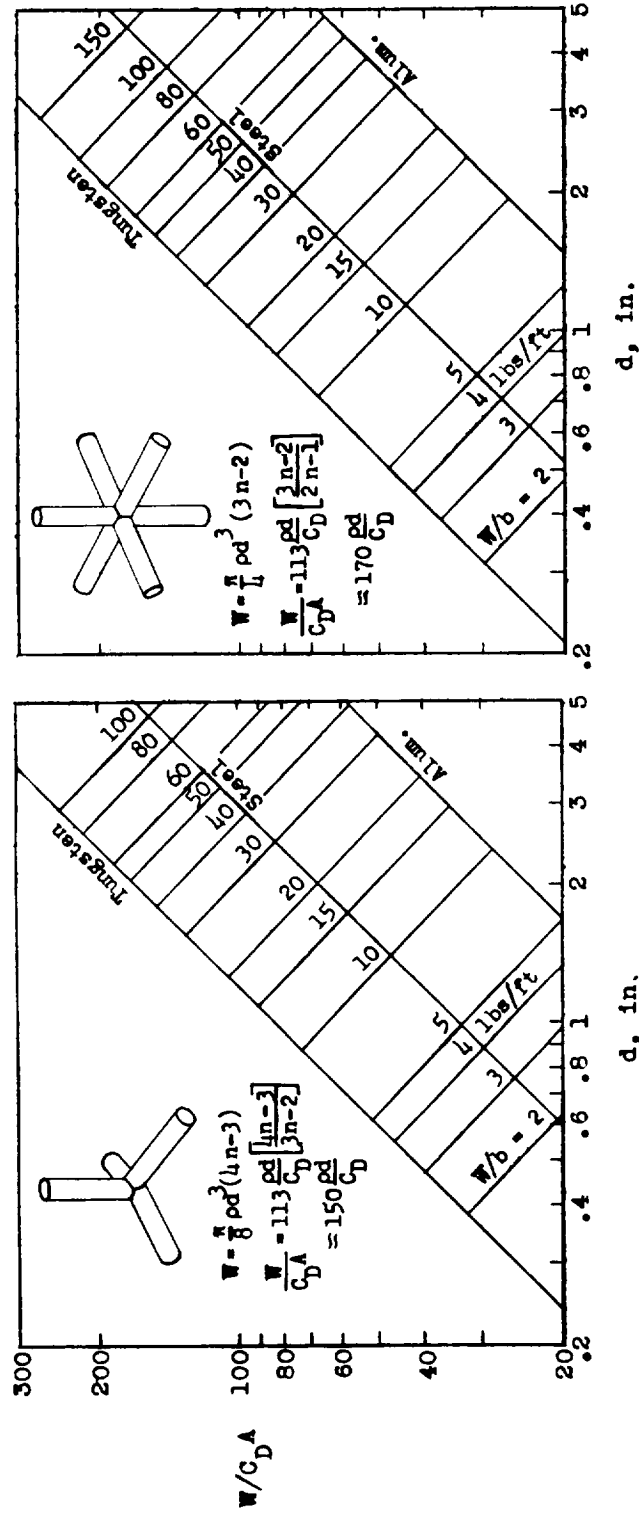Signal strength, db above noise

Figure 12.- Summary of radar test results; relative signal strengths of various radar targets at 8,000 yards range. S-band radar; λ = 4.22 inches.

(b) Six-leg jack.

$$W = \frac{\pi}{4} \rho d^3 (3n-2)$$

$$\frac{W}{C_D A} = 113 \frac{\rho d}{C_D} \left[\frac{3n-2}{2n-1} \right]$$

$$\approx 170 \frac{\rho d}{C_D}$$

(a) Four-leg jack.

$$W = \frac{\pi}{8} \rho d^3 (4n-3)$$

$$\frac{W}{C_D A} = 113 \frac{\rho d}{C_D} \left[\frac{4n-3}{3n-2} \right]$$

$$\approx 150 \frac{\rho d}{C_D}$$

Figure 13.- Estimated range of $\left(W/C_D A \right)$ and weight penalty for various decoy configurations of unit span; $C_D = 1.25$; $n \geq 5$.

$$W = \frac{3}{4}\pi\rho d^3[\pi(n-1)-2]$$

$$\frac{W}{C_D A} = 207\frac{\rho d}{C_D}\left[\frac{n-1.64}{n-1.58}\right]$$

$$\approx 207\frac{\rho d}{C_D}$$

(d) Three-ring decoy.

$$W = \frac{\pi}{2}\rho d^3(6n-7)$$

$$\frac{W}{C_D A} = 75\frac{\rho d}{C_D}\left[\frac{6n-7}{2n-3}\right]$$

$$\approx 226\frac{\rho d}{C_D}$$
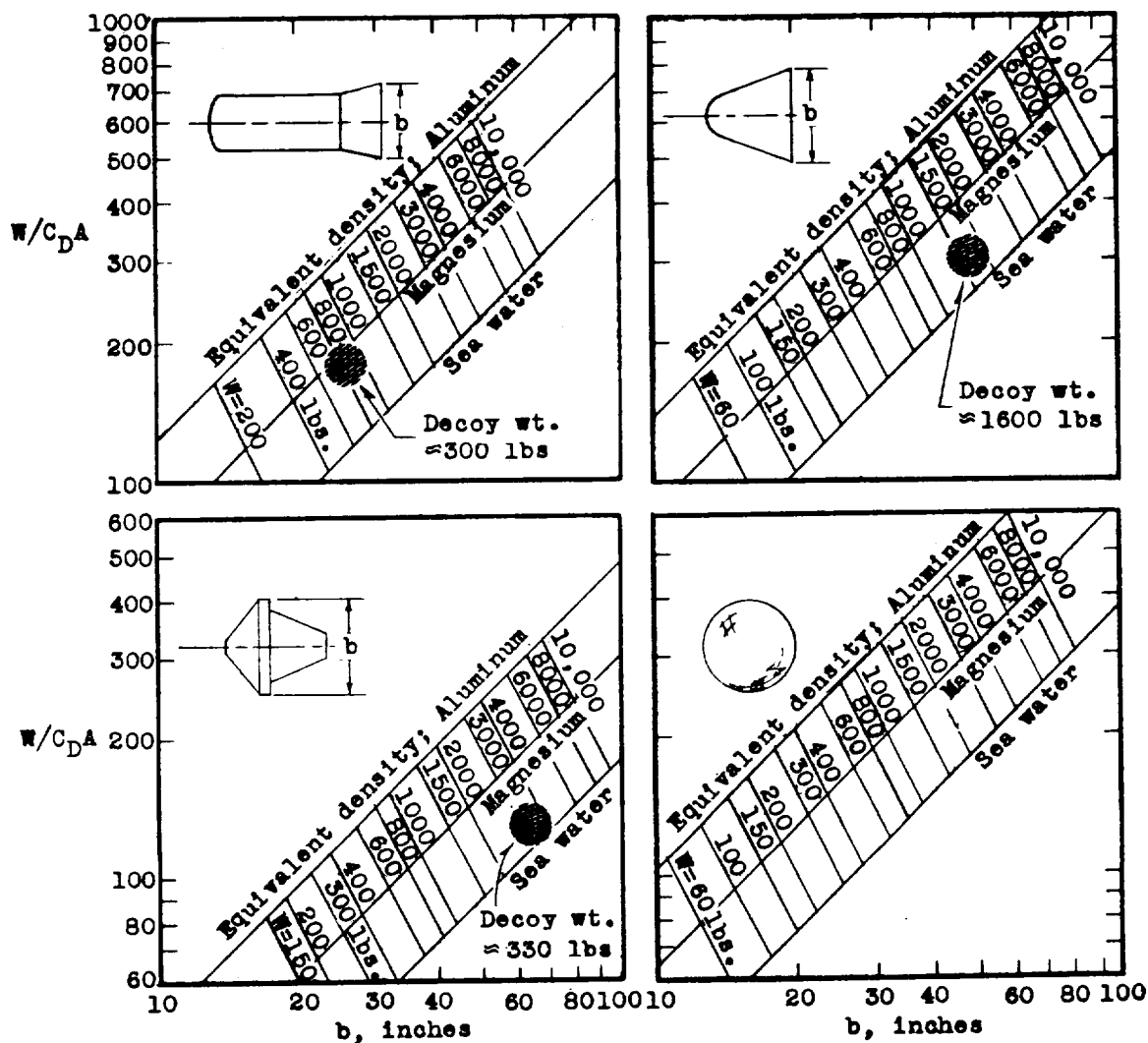
(c) 18-leg jack.

Figure 13.- Concluded.

Figure 14.- Estimated range of W/C_DA and weight penalty for various hypothetical warheads, showing areas of interest and 6-leg tungsten decoy weight penalty required to simulate reentry assuming S-band radar-detection devices; decoy span = 2b.